

Spatial organization and evolution period of the epidemic model using cellular automata

Liu Quanxing* and Jin Zhen†

*Department of mathematics, North University of China,
Taiyuan, Shan'xi, 030051, People's Republic of China*

(Dated: February 9, 2020)

We investigate epidemic models with spatial structure basing on the cellular automata method. The construction of the cellular automata is from Jörg R. Weimar's study about the reaction-diffusion equations (Phys. Rev. E 49). Here, It is shown that the spatial epidemic models exhibits spontaneous formation of dynamical patterns with fractal fronts (or resemble irregular spiral waves) at larger scales within the domain of chaos. Moreover the dynamical patterns with fractal fronts grows stably and exists periodically. The system also shows spatial period-2 structure at one-dimensional for certain parameter value. Simultaneity, in the domain of chaos the spatial period-2 structure will break and transition to spatial synchrony configuration.

PACS numbers: 05.50.+q, 87.23.Cc, 87.18.Hf, 89.75.Fb

I. INTRODUCTION

Several theoretical models have shown that population embed and disperse in space can be more stable than non-spatial counterpart in the ecology [1]. In oscillatory systems where the equilibrium is a limit cycle or more generally exists an unstable focus, diffusion or dispersal create wave-like patterns, the Lattice Lotka-Volterra (LLV) model was studied extensively [2, 3, 4]. The two most commonly seen patterns are spiral waves and turbulence. It has been shown that spirals play a very important role in ecological systems. For example, spatially induced speciation prevents extinction for the predator-prey models [5, 6]. A classical epidemic model is ordinary differential equations (ODEs), or called mean-field (MF) approximation [7]. The ODEs (or MF) mathematical approach to these problems deals with well mixed populations, where the subpopulations involved (typically susceptible, exposed, infected, and removed) interact in proportion to their sizes. Which is a non-spatial theory on pathogen evolution generally predicting selection for maximal number of secondary infectors, among those epidemic features, the existence of threshold values for the spread of an infection [8, 9]. A second classical approach describes spatially extended subpopulations, such as elements in a coupled map-lattice models [10]. In this, the geographic spread of an epidemic can be analyzed as a reaction-diffusion process. More recently, studies have shown large-scale spatiotemporal patterns in measles [11] and dengue fever [12]. These studies have shed new light onto key research issues in spatial epidemic dynamic, whereas about the detailed theoretical studies is difficulty. Recently, the study of population dynamics takes into account the species distribution in space, interactions between individual species that are located

in the same neighborhood, and mobility of the various species [13, 14, 15]. These studies predict the formation of spatial complex structure, phase transitions, multistability, oscillatory regions, etc. In the Ref. [15], the author studies the susceptible-infected-resistant-susceptible (SIRS) models with spatial structure using cellular automata rules, showing the formation process of the spatial patterns (turbulent waves and stable spiral waves) in the two-dimension space and existence a stable spiral waves in the SIRS model.

In this paper, we investigate the susceptible-exposed-infected-resistant (SEIR) model with spatial structure basing on the classical ODEs models [16, 17] using cellular automata arithmetic. In fact, many diseases are seasonal, and therefore an important question for further studies is how seasonality can influence spatial pathogen evolution. So, we consider the seasonal parameter, $\beta(t) = \beta_0(1 + \varepsilon \sin(2\pi t))$, where ε is the fluctuating amplitude of contact rate. Commonly, we describe the susceptibility, exposure, infection and recover process in terms of four nonlinear ODEs. We use S for susceptibles, E for the exposed, I for infectors, and R for the recovered. The dynamical equations for SEIR model are

$$\frac{dS}{dt} = \mu(1 - S) - \beta(t)IS, \quad (1a)$$

$$\frac{dE}{dt} = \beta(t)IS - (\mu + \delta)E, \quad (1b)$$

$$\frac{dI}{dt} = \delta E - (\gamma + \mu)I, \quad (1c)$$

$$\frac{dR}{dt} = \gamma I - \mu R, \quad (1d)$$

Where μ is the death rate per capita, $1/\delta$ and $1/\gamma$ are the mean latent and infectious periods of the disease. β is the rate of disease transmission between individuals. The population can be normalized to $S + E + I + R = 1$, so all dependent variables represent fractions of the population. In the original studies shown that the system

*Electronic address: liuqx315@sina.com

†Electronic address: jinzhn@263.net

of (1) exist three phase transition with respect to the fluctuating amplitude, ε , i.e stable behavior, limit cycle and chaotic behavior in the mean-field limit [16].

II. NEIGHBOURHOOD-DEPENDENT MODEL

Generally, studies on the spacial epidemic models show that there exists a spatial-temporal travelling wave [18] (e.g. dengue haemorrhagic fever (DHF) [12, 19] and measles [11]). However, few systems are well enough documented to detect repeated waves and to explain their interaction with spatial-temporal variations in population structure and demography. Actual epidemic spreading is spatial-temporal and local individual interact. Here we study the individual moving of the susceptible, exposed, infector and recover. Since in the CA model the individuals are considered here as mobile, they diffuse from one lattice site to another. Then the equations (1) read

$$\frac{\partial S(\mathbf{r}, t)}{\partial t} = \mu - \beta(t)IS - \mu S + D_1 \nabla^2 S(\mathbf{r}, t), \quad (2a)$$

$$\frac{\partial E(\mathbf{r}, t)}{\partial t} = \beta(t)IS - (\mu + \delta)E + D_2 \nabla^2 E(\mathbf{r}, t), \quad (2b)$$

$$\frac{\partial I(\mathbf{r}, t)}{\partial t} = \delta E - (\gamma + \mu)I + D_3 \nabla^2 I(\mathbf{r}, t), \quad (2c)$$

$$\frac{\partial R(\mathbf{r}, t)}{\partial t} = \gamma I - \mu R + D_4 \nabla^2 R(\mathbf{r}, t). \quad (2d)$$

We study the system (2) using cellular automata method which is suitable for modeling many reaction-diffusion systems in a quantitatively correct way basing on the Ref. [20], and demonstrate recurrent epidemic

spiral waves or traveling waves in an exhaustive spatial-temporal through the simulation. In simply we use $\mathbf{c}(\mathbf{r}, t)$ to denote the vector of local density individual in position \mathbf{r} and at time t , and $\mathbf{L}(\mathbf{c}(\mathbf{r}, t))$ to describe the local kinetics; \mathbf{D} is the diffusion coefficient matrix. Then the system (2) can be written as

$$\frac{\partial \mathbf{c}(\mathbf{r}, t)}{\partial t} = \mathbf{L}(\mathbf{c}(\mathbf{r}, t)) + \mathbf{D} \nabla^2 \mathbf{c}(\mathbf{r}, t). \quad (3)$$

In the following simulation, we may discard the equation (2d), since we concern the susceptible, exposed and infected.

We define this model as follows. Space is made up of a square lattice of $J \times J$ patches. In each step the individual randomly disperses in its neighborhood. The state of the cellular automata is given by a regular array of density vector \mathbf{c} residing on a two-dimension lattice. The central operation of the cellular automaton consists of calculating the sum

$$\mathbf{c}_i(\mathbf{r}, t) = \sum_{\mathbf{r}' \in N_i} \mathbf{c}_i(\mathbf{r} + \mathbf{r}'). \quad (4)$$

Where the summation takes up all of the nearest neighbors of the cell \mathbf{r} . The neighborhoods can be different for each species i . Here, we use the Moore neighborhood for all i in two dimensions. i.e.

$$N_{square} = \{(0, 0), (1, 0), (0, 1), (-1, 0), (0, -1), (1, 1), (-1, 1), (1, -1), (-1, -1)\}. \quad (5)$$

We normalize values of $\bar{\mathbf{c}}_i(\mathbf{r}, t) = \mathbf{c}_i(\mathbf{r}, t)/N_i$, the $\bar{\mathbf{c}}_i(\mathbf{r}, t)$ is local average density of the $\mathbf{c}_i(\mathbf{r}, t)$.

From the Ref. [20], the two-dimension discretization version of Eq. (3) takes the form

$$\mathbf{c}_i(\mathbf{r}, t + 1) = \mathbf{c}_i(\mathbf{r}, t) + \Delta t \mathbf{L}(\mathbf{c}_i(\mathbf{r}, t)) + D_{ii} \frac{\Delta t}{\Delta r^2} \nabla^2 \mathbf{c}_i(\mathbf{r}, t), \quad i = 1, 2, 3, 4. \quad (6)$$

Substituting the Eq. (4) into (6) and normalizing values of $\bar{\mathbf{c}}_i(\mathbf{r}, t)$ yield

$$\mathbf{c}_i(\mathbf{r}, t + 1) = \mathbf{c}_i(\mathbf{r}, t) + \Delta t \mathbf{L}(\mathbf{c}_i(\mathbf{r}, t)) + D_i \bar{\mathbf{c}}_i(\mathbf{r}, t), \quad i = 1, 2, 3, 4. \quad (7)$$

Where the

$$D_i = D_{ii} \frac{\Delta t}{\Delta r^2}, \quad i = 1, 2, 3, 4. \quad (8)$$

defines the space scale.

III. NUMERICAL RESULTS

We have performed extensive numerical simulations of the described model, and the qualitatively results shown here. In cellular automata simulation, periodic boundary conditions are used and $\Delta t = 0.005$. The space scale $D_1 = 0.2$, $D_2 = 0.05$, $D_3 = 0.02$, $D_4 = 0.2$ and grid size used in the evolutionary simulations is 100×100 cells. We have tested that the larger grid size does not change qualitative result for the evolutionary dynamics. The contact rate fluctuates with the seasons and can be approximated in several ways. For ease of exposition, we choose sinusoidal force, $\beta(t) = \beta_0(1 + \varepsilon \sin(2\pi t))$, where $0 \leq \varepsilon < 1$. Another more realistic option is term-time forcing, which

sets transmission rates high during school terms and low otherwise [21]. The spatial patterns are evolved from random initial condition and the maximum density of susceptible, exposed and infected equal to 0.5, 0.05 and 0.001 respectively, and the rest recover. Other initial conditions have been explored as well, and no changes have been observed in the behavior. In Fig. 1 and Fig. 3 four different snapshots during the temporal evolution of the system are presented in two dimensional. In those figure and hereafter the maximum density for the susceptible are depicted in white, the minimum density in black, and the middle density in gray.

Fig. 1 and Fig. 3 depict spatial patterns in the two-dimensional under different ε values (the fluctuating amplitude of contact rate) respectively. From evolution snapshots (Fig. 1(a)-1(d)), we see there is no occurrence of fractal fronts patterns even if the system reach a stable state for the fluctuating amplitude in certain interval. We turns out to be $\varepsilon^* < \varepsilon < \varepsilon_c$ for the parameter value used in the figure. Here the critical value ε_c is more than the value of the local dynamic of the chaotic point of system (1) [16], in which argument the critical value of $\varepsilon_c \approx 0.28$. However, we yields very different result for the critical value ε_c , which turns out to be $\varepsilon_c \approx 0.305$ for the parameter value used in the figure. As the ε ($\varepsilon > \varepsilon_c$, in the domain of chaos) increases and the evolution processes, the dynamical patterns with fractal fronts of spatial structures create (spirals waves), as time increase, become larger and more stable, and the local turbulence disappears (see the Fig. 3). The CA models are generally based on qualitative rather than quantitative information about the system. In order to quantitatively investigate the evolution of the system (2), we give the results using one-dimensional. For realizations on a one-dimensional CA model, a more explicit visualization of spatial organization within the lattice is provided by the space-time plot of Fig. 2 and Fig. 4.

We show in Fig. 2(a) part of three time series displaying the fraction of susceptible, exposed and infected randomly chosen in a patch for the first 10000 steps by CA. From the Fig.2(b)-2(d), it is clearly seen that the whole system shows the spatial period-2 structure when the ε between 0.048 to 0.305 (later we will introduce the ε small than a critical value ε^* case, and which turns out to be $\varepsilon^* \approx 0.048$ for the parameter value used in the Figure). Plot spatial-temporal pictures of the susceptible, exposed and infected respectively, where time increases from bottom to top and the horizontal axis represents the spatial location. The three time series of the susceptible, exposed and infected is self-sustained oscillations develop (see the Fig. 2(a)). These oscillations increase in amplitude respecting to the increase of fluctuating amplitude of the infection rate (compared the Fig. 2(a) and 4(a)). In fact, large oscillations will lead to (stochastic) extinction of the pathogens, when the value of fluctuating amplitude is more than ε_c , in the domain of chaos.

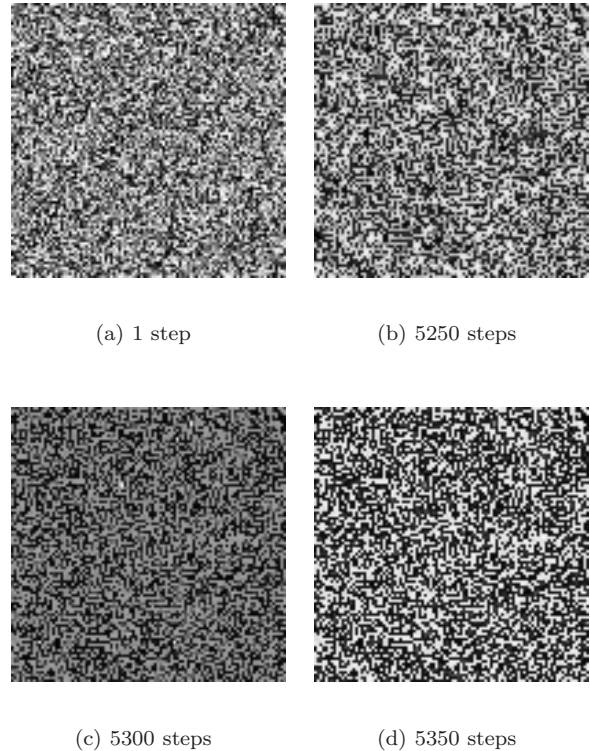


FIG. 1: A typical simulation shows four snapshots of the evolution in two-dimensional with the parameters $\mu = 0.02$, $\delta = 35.84$, $\gamma = 100$, $\beta_0 = 1800$ and $\varepsilon = 0.23$.

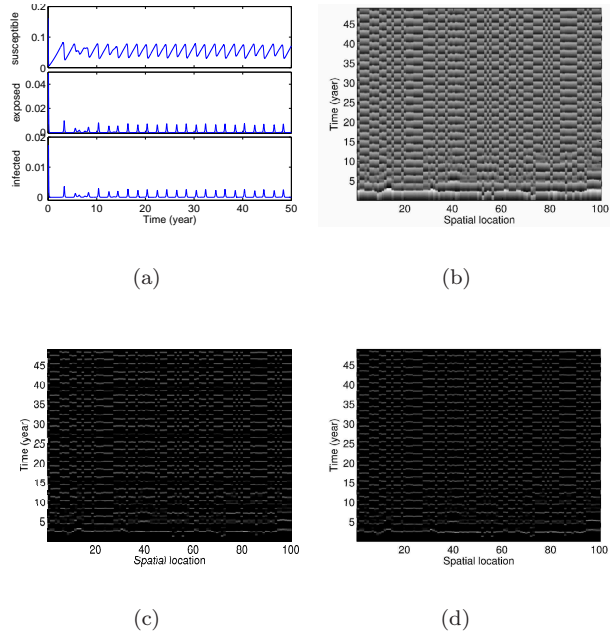


FIG. 2: The spatial period-2 structure results for the system (2) in one-dimension by cellular automata and the parameters are the same as those in Fig. 1.

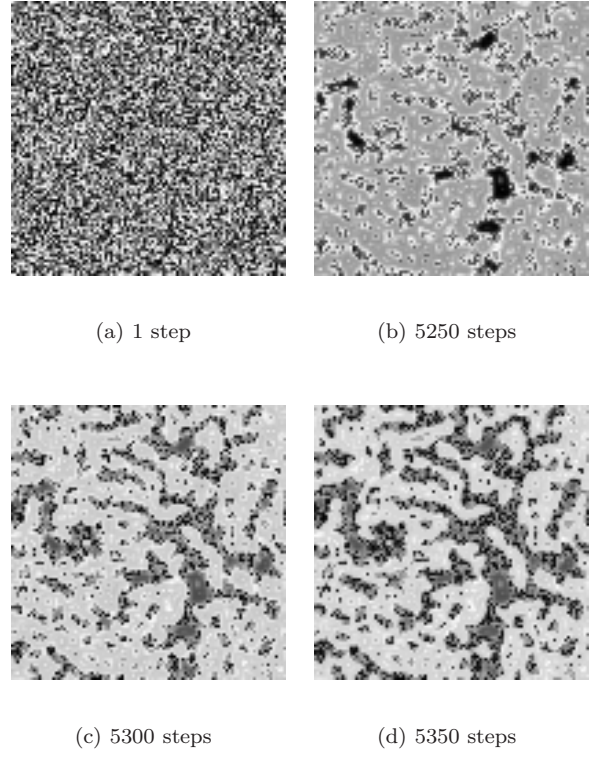


FIG. 3: A typical simulation shows four snapshots of the evolution in two-dimensional space. The same as in Fig. 1, $\mu = 0.02$, $\delta = 35.84$, $\gamma = 100$, $\beta_0 = 1800$ and $\varepsilon = 0.38$.

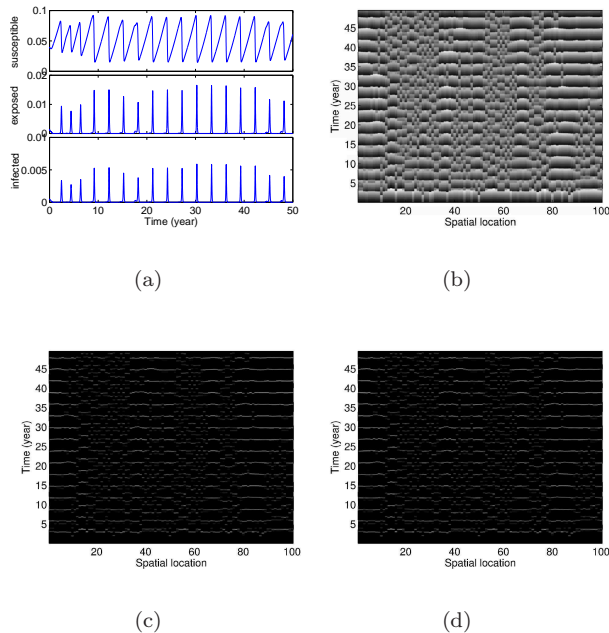


FIG. 4: The spatial period-2 structure results for the system (2) in one-dimension by cellular automata and the parameters are the same as those in Fig. 3.

To further investigate the impact of the fluctuating amplitude on the dynamical with fractal fronts (or spiral waves) and the spatial period-2 structure in two-dimensional and one-dimensional space respectively, we study the case where the SEIR model is deep in the domain of chaos and out of the chaos domain. We set $\varepsilon = 0.38$, the evolution of system (2) is shown in Fig. 3 and Fig. 4. Fig. 3(b)-3(d) three snapshots are taken at 5250, 5300 and 5350 steps respectively. These fractal front are broad and do not easily break, resulting in periodical recurrence of epidemic waves. In between local clusters and irregular waves, a region of turbulent waves exists. The spatial dynamics show that regularly recurrent infection waves are spiral waves with fractal fronts (Fig. 3(d)). Similarly the irregular spiral waves can also be observed even when the fluctuating amplitude is much more than the critical value ε_c . The results are not shown in this work. As these infection clusters grow, the availability of infected hosts per susceptible host is reduced, decreasing the number of new infectors.

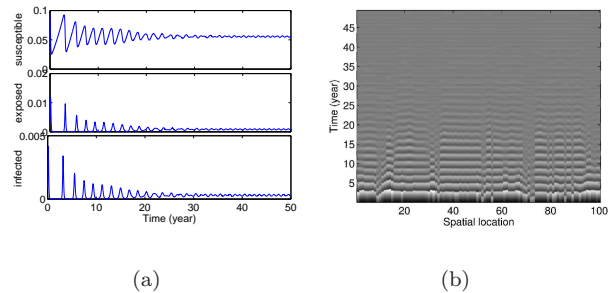


FIG. 5: The spatial-temporal evolution for the system (2) in one-dimension by cellular automata at $\varepsilon = 0.035$.

Figure 5 shows the time evolution of the density of the individuals and the spatial-temporal configurations for the system (2) at $\varepsilon = 0.035$. The spatial-temporal evolution for the expose and infected have the resemblance to the susceptible. It can be clearly noticed that spatial period-2 structure are disappear and the stationary state is a fixed point with decreasing ε . The situation corresponds to that of an endemic infection, with a low and persistent fraction of infection individuals as Fig. 5(a). The oscillations is decay to the fixed point at the ε small than the critical value ε^* case.

IV. CONCLUSIONS

In conclusion, we demonstrate the existence and persistence of recurrent infection waves in an exhaustive spatial-temporal. We have investigated the dynamical patterns with fractal fronts in system (2) in two-dimensional and coupled oscillations with the spatial period-2 structure. We show that within the domain of chaos (fluctuating amplitude $\varepsilon > \varepsilon_c$) dynamical patterns with fractal fronts (or spiral waves) recur periodically and the recurrence is insensitive to the change of the fluctuating amplitude ε . Moreover the dynamical patterns with fractal fronts grows stably and exists periodically. The system also shows spatial period-2 structure at one-dimensional when the control parameter ε more than ε^* . Simultaneity, in the domain of chaos the spatial period-2 structure will break and transition to spatial synchrony configuration.

Acknowledgments

This work is supported by the National Natural Science Foundation of China under Grant No 10471040.

-
- [1] P. Rohani and O. Miramontes, Proc. Roy. Soc. Lond B **260**, 335 (1995).
- [2] A. Provata and G. A. Tsekouras, Phys. Rev. E **67**, 056602 (2003).
- [3] G. A. Tsekouras and A. Provata, Phys. Rev. E **65**, 016204 (2001).
- [4] A. Provata, G. Nicolis, and F. Baras, J. Chem. Phys. **110**, 8361 (1999).
- [5] J. S. Nicholas and P. Hogeweg, Proc Roy. Soc. Lond. B **265**, 25 (1998).
- [6] W. S. C. Gurney, A. R. Veitch, I. Cruickshank, and G. McGeachin, Ecology **79**, 2516 (1998).
- [7] J. D. Murray, *Mathematical Biology* (Springer-Verlag Berlin Heidelberg, 1993).
- [8] R. M. Anderson and R. M. May, Nature **318**, 323 (1985).
- [9] R. M. Anderson and R. M. May, Science **215**, 1053 (1982).
- [10] U. Dieckmann, R. Law, and J. A. J. Metz, *The Geometry of Ecological Interactions: Simplifying Spatial Complexity* (Cambridge University Press, United Kingdom, 2000).
- [11] B. T. Grenfell, O. N. B. Arnstad, and J. Kappey, Nature **414**, 716 (2001).
- [12] D. A. T. Cummings, N. E. Huang, T. P. Endy, A. Nisalak, and B. D. S. K. Ungchusak, Nature **427**, 344 (2004).
- [13] T. Antal, M. Droz, A. Lipowski, and G. Ódor, Phys. Rev. E **64**, 036118 (2001).
- [14] M. Droz and A. Pekalski, Physica A **298**, 545 (2001).
- [15] W. M. van Ballegoijen and M. C. Boerlijst, Proc. Natl. Acad. Sci. **101**, 18246 (2004).
- [16] L. F. Olsen and W. M. Schaffer, Science **249**, 499 (1990).
- [17] B. T. Grenfell, A. Kleczkowski, S. P. Ellner, and B. M. Bolker, Phil. Trans. Roy. Soc. Lond. A **348**, 515 (1994).
- [18] S. Djebali, Nonl. Anal.: Real World Applications **2**, 417 (2001).
- [19] A. Vecchio, L. Primavera, and V. Carbone, Phys Rev E **73**, 1913 (2006).
- [20] R. J. Weimar and B. Jean-Pierre, Phys. Rev. E **49**, 1749 (1994).
- [21] J. D. E. David, P. Rohani, M. B. Benjamin, and B. T. Grenfell, Science **287**, 667 (2000).